MODELLING OF SPACECRAFT PLASMA ENVIRONMENT INTERACTIONS

Jean-François ROUSSEL

ONERA/DESP, 2 Av. Edouard Belin, 31055 Toulouse Cedex, France; roussel@onecert.fr

***Abstract** : The available methods for modelling spacecraft plasma interactions are reviewed. Analytic equations describing the physics and numerical solving methods are discussed. The cases of spacecraft in GEO, in LEO, and in presence of electric propulsion are more specifically addressed.*

1. Introduction

The modelling of spacecraft plasma interactions is a vast domain. The first aim of that course will be to provide a general view of the available methods in that field. The second shall be to provide more practical information on some of those methods of particular interest.

Concerning its domain of application the scope of that course shall be limited to quasi-static charging of spacecraft. Wave propagation or transient phenomena like the development of an electrostatic discharges are thus excluded, but all types of plasma environment will be addressed, with a specific emphasis on GEO, LEO and Electric Propulsion environments (section 4). Concerning the modelling methods, the scope will be rather large: from the theoretical basis (section 2.1) of the equations to their possible simplifications in practice (section 2.2) and finally the numerical solving methods (section 3). Concerning the audience, that course primarily aims at modellers, but experimenters can learn something about what modellers do (some of them may also go directly to section 4 for specific situation studies).

2. Modelling: from the physics to the equations

The first step in any simulation, is to represent the physics through equations. The physics shall dictate which kind of equations are to be used, and how far they can be simplified. The general equations are discussed first, and simplifications possible in usual flight conditions are addressed next.

2.1. The theoretical side: general equations

The fundamental equations necessary to represent the particles (or matter) and fields involved in a plasma dynamics are recalled here, to establish a solid basis to a self-contained view of spacecraft plasma interaction modelling.

2.1.1. The matter

The material particles constitutive of space plasma are mainly electrons, protons and positive ions. They cannot in general be considered as thermalised and having a Maxwellian distribution. They must be described following a kinetic approach, also called microscopic, in contract to the fluid or macroscopic approach (Euler or Navier-Stokes equations). The number dN_i and dN_e of ions and electrons with space co-ordinate $\vec{x}$, up to d^3x, and with velocity $\vec{v}$, up to d^3v, are given through the ion and electron distribution functions $f_i(\vec{x},\vec{v},t)$ or $f_e(\vec{x},\vec{v},t)$ in phase space (3D of space, 3D of velocity space, at a given time) by:

$$dN_{i/e} = f_{i/e}\, d^3x\, d^3v \tag{1}$$

The evolution of those distribution functions are ruled by the following Boltzmann equation:

$$\frac{\partial f_{i/e}}{\partial t} + \vec{v}.\frac{\partial f_{i/e}}{\partial \vec{x}} + \frac{q_{i/e}}{m_{i/e}}\left(\vec{E} + \vec{v}\times\vec{B}\right).\frac{\partial f_{i/e}}{\partial \vec{v}} = \text{ collision term} \tag{2}$$

where the right hand side term accounting for elastic or reactive collisions depends on the type of collisions. That equation is called Vlasov equation in the absence of collisions, Fokker-Plank equation for a Coulomb type collision term, while the Boltzmann equation name is most often used for neutral species without electromagnetic force. When the collision terms are inelastic (ionisation, charge exchange, reactions, excitations), several species, some of them possibly neutral, are to be taken into account, each with its own distribution function.

2.1.2. The fields

The general field equations are the well known Maxwell equations:

$$\vec{\nabla}.\vec{E} = \rho/\varepsilon_0 \quad \text{(Poisson Eq.)} \tag{3}$$

$$\vec{\nabla}\times\vec{E} = -\partial\vec{B}/\partial t \quad \text{(Faraday Eq.)} \tag{4}$$

$$\vec{\nabla}.\vec{B} = 0 \quad (B \text{ divergence Eq.}) \tag{5}$$

$$\vec{\nabla}\times\vec{B} = \mu_0\left(\vec{j} + \varepsilon_0\partial\vec{E}/\partial t\right) \quad \text{(Ampère Eq.)} \tag{6}$$

with the charge and current densities ρ and $\vec{j}$ coming from matter distribution functions through

$$\rho(\vec{x},t) = \sum_{\text{species } s}\int d^3v\ q_s\ f_s(\vec{x},\vec{v},t) \tag{7}$$

$$\vec{j}(\vec{x},t) = \sum_{\text{species } s}\int d^3v\ q_s\ f_s(\vec{x},\vec{v},t)\vec{v} \tag{8}$$

Maxwell equations are given here in vacuum since the reactions of the matter to the fields are included in the charge and current densities. This is the "charges in vacuum" description.

Another description is the dielectric description, which is of common use for electromagnetic propagation in a material medium. It consists in solving the equations of motion for matter in reaction to the fields and putting the result in the form of a dielectric constant ε_r in Maxwell equations. However the equations of motions cannot be analytically solved in their general form (2) and some assumptions are necessary to get a dielectric constant (fluid approach, cold plasma, linearisation…). This description lacks thus of generality to be described here. In practice it is mostly used to model the propagation of waves in plasma. In such a case linearising the equations of motion is often unavoidable and the separation of the different modes (frequencies) allows to compute a well defined dielectric constant. In the opposite static case, a plasma screens constant electric fields, which makes the dielectric constant of plasma infinite at zero frequency, and thus the dielectric description unusable.

2.1.3. The Boundary Conditions

The space environment is an infinite medium (or almost…) but computation boxes are finite. That forces the modeller to define at the external boundaries of his simulation box, both the fields (in fact their normal component or some other mathematically consistent component) and the matter fluxes. The boundary conditions also require a specific treatment at the boundaries of the objects or spacecraft (S/C) embedded in the plasma.

2.1.3.1. External boundary conditions: the environment

The general principle is to have a computation box large enough for the perturbation of the natural environment due to S/C to be negligible. The external boundaries are then simply described as the natural unperturbed environment. This is the situation described in the present general section. That idyllic situation is however not always reachable, and specific boundary conditions are to be considered. Some cases shall be addressed later in 2.2.3.1.

Concerning matter, the required boundary conditions are fluxes incoming into the computation box. Consistently with the kinetic approach, a microscopic description of those fluxes is needed. The "microscopic flux" incoming through a boundary surface of incoming normal $\vec{n}$ is given by the "flux distribution":

$$\vec{v}.\vec{n}\ f_{i/e}(\vec{x},\vec{v},t)\ \mathrm{H}(\vec{v}.\vec{n}) \tag{9}$$

where $\mathrm{H}(x)$ is Heaviside step function (1 for $x>0$, 0 for $x<0$). That microscopic description requires lots of information for velocity distribution of particles in the space environment, and will often be simplified (isotropic, or Maxwellian distributions, see 2.2.3.1 below).

Concerning the fields, the ambient electric field is usually zero because of plasma screening (at least at S/C scale). In a frame moving with S/C, an electric field $\vec{v}\times\vec{B}$ exists when magnetic lines are crossed. It is however negligible in GEO and small in LEO (of the order of 0.3 V/m).

On the contrary, the earth magnetic field may be important in some simulations. In the general framework presented here it is to be considered as boundary conditions to be propagated inside the computation box through Maxwell equations, but in practice, due to the linear character of Maxwell equations, that ambient magnetic field is usually considered as a uniform "background" field to be added to the local fields in the simulation.

2.1.3.2. Boundary conditions for the objects: spacecraft modelling

The charging will be limited here to surface charging. One must be aware that in reality, the plasma charges and fields do not stop at the surface of embedded objects. Energetic particles may go through the S/C coatings and then into internal devices (cable insulators, electronic devices…). That physics covers the large domains of deep dielectric

charging, particle transport in matter, dose deposition, singular events, etc. This course shall however be limited to lower energy plasma (below 10-100 keV), which is stopped by the first microns of coatings.

The matter fluxes, or currents as far as charge fluxes are concerned, are thus considered to be collected by S/C surfaces. Those oncoming fluxes create outgoing fluxes of particles re-emitted by surfaces. A non exhaustive list of phenomena can be given:

- Electrons produce secondary electrons
- Ions produce secondary electrons
- Energetic ions sputter materials and produce atoms or ions
- Photons produce photo-electrons

Their relative importance is variable. Secondary emission and photo-emission are major phenomena in GEO charging, sputtering is important in electric propulsion, etc. The yields of these effects and the distribution functions of the emitted particles are usually taken from experiments. Physical microscopic models of those phenomena (cascade of collisions in the materials e. g.) do exist, but usually have a reduced predictive character.

Those collected and emitted currents result in surface charge $\sigma(\vec{x},t)$ build-up on S/C surfaces

$$\frac{d\sigma}{dt}(\vec{x},t) = \sum_{\text{species } s} \int d^3v \; \vec{v}.\vec{n}\, q_s \; f_s(\vec{x},\vec{v},t) \tag{10}$$

for all species *s* of charge q_s. That is to be translated in electric field and/or potential boundary conditions on S/C. A basic approach could be to solve Poisson equation outside and inside spacecraft taking into account charges both on S/C surfaces and outside S/C, skipping thus the issue of electrical boundary conditions on S/C. This approach is however intractable in practice for two main reasons: dielectric coatings on metals create very thin capacitors (typically 100 µm) that would require a meshing at that microscopic scale, and the computation of image charges on conductors adds an extra difficulty. We shall discuss below (2.2.3.2) a practical approach.

The electric charges on spacecraft may also redistribute internally to the S/C through some conductivity. Surface and volume conductivities are thus to be taken into account. They can also be enhanced through dose (rate) or UV flux. Those data are also mainly taken form experimental measurements.

Magnetic field boundary conditions on S/C surfaces are usually easier to handle since they are due to current loops in S/C, that are known from S/C design. They show up in case of wave emissions (coupled electromagnetic conditions for antennas or tubes) or e. g. for Hall thrusters (static magnetic field of thruster). Things get more involved in case of electrostatic discharge, since a full electromagnetic model of the coupling of S/C electrical structure must be performed. It is yet beyond the scope of that course that is limited to surface effects concerning spacecraft.

2.2. The practical side: possible simplifications - difficulties

2.2.1. The matter

The general Boltzmann kinetic equation (2) given in 2.1.1 is very costly to solve. Working in high dimensional phase space (6D in general) is costly, but computing accurate collision or interaction terms may be even more (right hand side of (2), not explicitly written).

That approach is thus simplified as soon as it proves possible. A key parameter is the collision/interaction frequency, or mean free path. For very low or zero collision frequency no collisions are modelled and Eq. (2) reduces to Vlasov equation

$$\frac{\partial f_{i/e}}{\partial t} + \vec{v}.\frac{\partial f_{i/e}}{\partial \vec{x}} + \frac{q_{i/e}}{m_{i/e}}\left(\vec{E} + \vec{v}\times\vec{B}\right)\frac{\partial f_{i/e}}{\partial \vec{v}} = 0 \tag{11}$$

This is often applicable to ions, since they are little affected by collisions with electrons.

On the contrary, when collisions are frequent (compared to transit times), local thermal equilibrium is achieved. One can then assume that velocity distributions are Maxwellian

$$f_{i/e}(\vec{x},\vec{v},t) = \left(\frac{m_{i/e}}{2\pi k_B T_{i/e}(\vec{x},t)}\right)^{3/2} e^{-\frac{m_{i/e}(\vec{v}-\vec{u}(\vec{x},t))^2}{2k_B T_{i/e}(\vec{x},t)}} n_{i/e}(\vec{x},t) \tag{12}$$

perfectly described by their first three moments, density *n*, mean velocity $\vec{u}$ and temperature *T* (which are local). The dynamics is then ruled by fluid equations that are obtained by integration of the moments of Boltzmann equation (2): the continuity equation for zero order moment (simply integrate (2) over d^3v)

$$\frac{\partial n_{i/e}}{\partial t} + \vec{\nabla}.\left(n\vec{u}_{i/e}\right) = 0 \tag{13}$$

and the momentum equation for first order moment of (2) (multiply (2) by $\vec{v}$ and integrate over d^3v), equivalent to Euler or Navier-Stokes equation for charged particles

$$m_{i/e}n_{i/e}\left[\frac{\partial \vec{u}_{i/e}}{\partial t} + \left(\vec{u}_{i/e}.\vec{\nabla}\right)\vec{u}_{i/e}\right] = q_{i/e}\left(\vec{E} + \vec{u}_{i/e}\times\vec{B}\right) - \vec{\nabla}.\vec{\vec{P}}_{i/e} \tag{14}$$

with a possible extra term for collisions with another species. The pressure tensor or scalar $P_{i/e}$ has to be obtained from medium state equation ($P = nkT$, e. g. with isothermal hypothesis, or an extra energy transport equation from second moment of (2)).

Electrons can sometimes be considered in that situation of local thermal equilibrium.

They can first be thermalised due to a large collision frequency, either with neutrals or ions. Typical collisions frequencies are estimated in the table below for ionosphere and magnetosphere typical densities and temperatures from the following collision frequencies given in MKSA units [Quémada]:

$$\nu_{e\text{–}ion} \approx 3\times10^{-5} n_{ion} T_e^{-3/2} \tag{15}$$

$$\nu_{e\text{–}neutral} \approx 10^{-15} n_{neutral} T_e^{1/2} \tag{16}$$

Electrons can thus be considered as thermalised in ionosphere after a fraction of second, but not necessarily within the transit time in a spacecraft vicinity (below 1 ms).

	Ionosphere	Magnetosphere
n_{ion}	10^{10}-10^{12} m^{-3}	10^{6}-10^{7} m^{-3}
$n_{neutral}$	10^{12} to 10^{16} m^{-3}	-
T_e	1000 K	1 eV
$\nu_{e\text{-}ion}$	10-1000 s^{-1}	10^{-4} s^{-1}
$\nu_{e\text{-}neutral}$	0.1 to 100 s^{-1}	-

Table 1 – Orders of magnitude of electron collision frequency

It was however observed experimentally that many plasma exhibit Maxwellian distribution in spite of very low computed collisions frequencies. This is Langmuir paradox. Its origin lies in other sources of thermalisation like plasma-wave interactions, gyration in magnetic field, etc. Wave-particle interactions are for example thought to be the source of solar wind observed thermal character, in spite of a collision mean free path larger than sun-earth distance.

In some cases, an even stronger simplification can be achieved. When thermal equilibrium is achieved not only locally but also globally, particles follow the global Maxwell-Boltzmann distribution of thermal equilibrium

$$f_e\left(\vec{x},\vec{v},t\right) = \left(\frac{m_e}{2\pi k_B T_e}\right)^{3/2} e^{-\frac{m_e\vec{v}^2/2 - e\phi\left(\vec{x},t\right)}{k_B T_e}} n_0 \tag{17}$$

which reduces to Boltzmann distribution for densities

$$n_e\left(\vec{x},t\right) = n_0\, e^{\frac{e\phi\left(\vec{x},t\right)}{k_B T_e}} \tag{18}$$

for a local potential distribution $\phi\left(\vec{x},t\right)$.

This is a tremendous simplification that is thus to be used as soon as it proves possible. Solving fluid equations (13) and (14) in 3D is faster than solving kinetic equations (2) or (11) in 6D, but getting a direct analytical solution (17) and (18) is even better. Moreover it avoids any time integration at electron dynamics time scale, which is usually overwhelmingly costly. Let us remark that Boltzmann distribution can also be obtained from fluid equation (14) by neglecting electron inertia ($m_e \to 0$), and assuming the electric field derives from a potential (electrostatic assumption).

The conditions of validity of that Boltzmann distribution are thus very important. From its "global thermal equilibrium derivation", it is clear that they are the conditions of a closed system at thermal equilibrium:

- a single system (no potential barrier)
- enough time to reach equilibrium
- closed: no (important) losses.

The last point is sometimes translated as “no positive potentials on the spacecraft” (potential reference being the bulk plasma), which is somewhat inaccurate. There could be for example somewhere a grid with positive potential but collecting no charges (infinite transparency) and its potential energy well would be filled accordingly to (18) when thermalisation is achieved. On the contrary some electrons are collected by the negatively floating surfaces of a spacecraft (the tail of the distribution function) and the electron distribution in the sheath is not perfectly Maxwell-Boltzmann (the tail of outgoing electrons is truncated).

However, since surfaces at a positive potential not collecting electrons yet, are rare, and since the losses on surfaces at (floating) negative potential are small, the condition “no positive potentials on the spacecraft” is not so bad. Moreover, even though the Boltzmann distribution is inaccurate for electron density in the sheath, the current collected on the surface

$$j_e(\vec{x},t) = en_0 e^{\frac{e\phi(\vec{x},t)}{k_B T_e}} \sqrt{\frac{k_B T_e}{2\pi m_e}} \tag{19}$$

that can be derived from Maxwell-Boltzmann distribution is exact (from Liouville theorem that says that distribution functions are unchanged along phase space trajectories, hence if particles with enough total energy are not prevented to reach the surface by a potential barrier, they do reach it, and integrating over them gives (19), which is correct). It is even exact if thermalisation within the computation box is insufficient, but that the distributions of electrons entering it are Maxwellian (same reasons). Those are the reasons of the great success of Boltzmann distribution in plasma modelling.

Let us finally note that ions are usually not in this situation of global thermal equilibrium (this is why only the electron subscript *e* was noted here): they are in a directional supersonic flow in LEO (which leads e. g. to the non equilibrium wake phenomenon) contrary to the subsonic quasi-isotropic flow of electrons. Moreover, the negative floating potential of spacecraft makes the closed system assumption invalid for ions.

2.2.2. The fields

The magnetic field induced by plasma is usually small. Although plasma is diamagnetic and reduces any magnetic field through electron gyration, that effect is very small. It is in particular much less efficient that electric potential screening (if such a comparison can be done). So the magnetic field induced by plasma currents through Ampère law (6) is usually negligible and not considered.

The plasma induced magnetic field may yet be important in some very specific cases. In solar wind ambient magnetic field is much lower that around earth, and the plasma induced magnetic field is no more negligible. During electrostatic discharges currents are large, displacement currents (second term in the right hand side of Ampère Law (6)) are also large, and often larger due the rapidity of the phenomenon, which may induce important magnetic fields. The propagation of high frequency electromagnetic waves in plasmas also involved magnetic counter-reactions. Those cases shall not be treated in the scope of that course yet.

The major field of interest is thus the electric field, and it may even most of the time be treated in the electrostatic approximation: the electric field has zero rotational (no *B* variation in Faraday law (4)), and is thus the gradient of an electrostatic potential.

2.2.3. The boundary conditions

2.2.3.1. External boundary conditions: the environment

In the framework of a microscopic, or kinetic, modelling the microscopic particle fluxes are to be entered at the boundaries. The cold plasma that exists at all altitudes with variable density is an approximately thermalised Maxwellian plasma (see typical densities in table 1, above), also approximately at rest (there are some “winds” in the ionosphere yet). The fluxes to be injected are thus Maxwellian fluxes (half-Maxwellian). Since the spacecraft velocity is always negligible with respect to electron velocities, they are Maxwellian at rest for electrons. On the contrary S/C velocity is (much) larger than ion velocities in LEO, and the injected Maxwellian distributions are to be shifted by S/C velocity, which gives a microscopic flux through a boundary of incoming normal $\vec{n}$:

$$\sim \vec{v}.\vec{n}\, e^{-\frac{m_i(\vec{v}-\vec{u}_{S/C}(\vec{x},t))^2}{2k_B T_i(\vec{x},t)}} H(\vec{v}.\vec{n}) \tag{20}$$

In case of Monte Carlo simulations discussed below, the random generation of such ions may be impossible with direct analytical methods when $\vec{v}.\vec{u}_{S/C}$ is not zero. That small difficulty may be circumvented by the approximation $\vec{v}.\vec{n} \sim \vec{u}_{S/C}.\vec{n}$ since microscopic velocities are close to average velocity at large mach number *M* (correct for O+ at *M* ~10 but not for H+ at *M* ~ 2), or by other random generation techniques (numerical integration of the partial probability function, or rejection methods).

More energetic electrons are also to be taken into account: trapped electrons in radiation belts and precipitating electrons in the auroral zones. While the former have an approximately isotropic distribution function, the auroral electrons rather have velocities along magnetic field lines, which must be properly modelled.

The fluxes discussed so forth are conform to the idyllic image of an unperturbed plasma at mesh boundary presented in 2.1.3.1. The external boundary conditions for potential or electric field in such a framework can simply be zero electric potential at all boundaries (Dirichlet conditions), or zero electric field at some boundaries (Neumann conditions).

But things are not as simple, since the perturbation generated by a spacecraft only vanishes asymptotically. For example, the negative floating potential of a body in a plasma at rest, after an exponential decay in the sheath, only vanishes following a $1/r^2$ law in the pre-sheath [Bernstein and Rabinowitz]. That can be easily understood if one considers that at a distance r from the body of radius r_0, ion density is reduced by a factor $1-r^2/r_0^2$ (no ions are coming from the solid angle covered by the body). Equating that ion density with electron (linearised) Boltzmann density gives a potential decay in $1/r^2$ in the pre-sheath. That kind of mixed boundary conditions can be implemented through their homogeneous form:

$$\vec{E}_{boundary}.\vec{n} = \phi_{boundary}\frac{2\vec{r}.\vec{n}}{r^2} \tag{21}$$

that are correct mixed Dirichlet-Neumann boundary conditions.

2.2.3.2. Boundary conditions for the objects: spacecraft modelling

The boundary conditions on S/C surfaces are straightforward concerning matter modelling: ions and electrons impinging fluxes are collected and other secondary fluxes are re-emitted accordingly to the physical phenomena listed discussed in 2.1.3.2 (with yields and distribution function yet to be known, most of the time from experiments). The impinging fluxes may be simplified by thermal equilibrium hypotheses consistently with the matter modelling in volume.

The major issue resides in electric field boundary conditions. The integration of collected and emitted currents gives surface charge, but the resolution of Poisson equation requires potential or electric field conditions on surfaces. The relation between charges and potentials is given by capacitances. However plasma and sheaths are non linear and there is thus no linear relationship between the charge on a S/C and its potential, since the extension of the sheath varies with the potential.

In the absence of plasma yet, the physics is governed by Laplace equation (Poisson Eq. without charge), which is homogeneous (no 2nd member). Hence the potential to charge relation is linear and the capacitance of a spacecraft in vacuum is constant

$$Q_{sat} = C_{sat}\phi_{sat}$$

and can be computed, as e. g.

$$C_{sat} = 4\pi\varepsilon_0 R$$

for a spherical body of radius R (typically hundreds of pF for S/C in GEO).

In presence of a plasma, the relation between charge and potential is only linear for a fixed charge density. The practical method to determine a S/C potential is to find the solution ϕ of Poisson equation (3) as the sum of an arbitrary solution ϕ_1 of the inhomogeneous equation (3) and a solution ϕ_2 of the homogeneous Laplace equation, normalised so as to account for the right charge Q on S/C (the result of the dynamics at a given time):

1. Solve Laplace equation (once for all) and normalise the solution ϕ_2 so that the charge on spacecraft is unity (through Gauss theorem, the integral form of Poisson Eq.).
2. Solve Poisson equation (at each time step) with the right charge density (at that time step) but an arbitrary fixed potential on S/C.
3. Applying Gauss theorem to that solution ϕ_1 gives the corresponding arbitrary charge on S/C, Q_1.
4. The correct solution is $\phi = \phi_1 + (Q - Q_1)\,\phi_2$: it verifies inhomogeneous Poisson equation, and accounts for the right charge Q on S/C.

Let us also note that, if only homogeneous boundary condition were used at mesh external boundaries (Dirichlet, Neumann, or mixed like (21)) all ϕ_1, ϕ_2 and ϕ verify them. If non homogeneous boundary conditions (e. g. ϕ_{boundary} = given constant) are to be used, they must be used for ϕ_1 only.

That was the simple case of an equipotential S/C. A first complication arises for more realistic non equipotential S/C. The charge on surface dielectric is local and has to be translated in local potentials. The general principle is to use

Green functions, i. e. solutions of Poisson equation with a local charge only (vacuum in volume and no charge on the rest of the surfaces). They are the equivalent of ϕ_2 solution of Poisson homogeneous equation (Laplace) with a singular charge on a S/C point (instead of a global charge on S/C).

General Green function formalisms involves Dirac singular distributions (for local charge) and we shall thus immediately consider the spacecraft surfaces as discretised (meshed) in that sub-section in order to avoid that complication. For a discretised S/C surface the Green functions are the solutions of Poisson homogeneous equation with only a unity charge on a point of the surface mesh. Doing that for each surface point allows to compute column by column the inverse capacitance matrix D relating potentials to charges

$$\phi_i = \sum_{\text{surface mesh points } j} D_{ij} Q_j \tag{22}$$

The capacitance matrix C relating the charges to the potentials

$$Q_i = \sum_j C_{ij} \phi_j \tag{23}$$

is the inverse of that D matrix. Those computations are the equivalent of the point 1 above for equipotential S/C. The general procedure is still the same:

1. Compute capacity matrix
2. Solve inhomogeneous Poisson equation (3) with the right charge density but arbitrary potentials on S/C.
3. Determine the corresponding arbitrary charge on S/C, Q_1 (local now).
4. The correct solution is $\phi = \phi_1 + D.(Q - Q_1)$ for potentials on S/C (a correct track of potentials in volume is to be kept from each computation to determine D matrix, for example in a rectangular D matrix).

The second and last step to realistic spacecraft is to take into account thin capacitors constituted by S/C coatings (coverglasses, paints…) over grounded structure. Applying the general scheme just described would require meshing at the scale of those coatings (typically 100 μm), which is unrealistic. Those capacitors are thus to be taken into account explicitly. The general method consists simply in distributing the charges on all surfaces consistently with the capacitor network, with opposite charges on corresponding capacitor electrodes (relative charging). The differential potentials are deduced from those capacitor charging. There remains then to distribute the overall S/C charge (global charging) over all the external surfaces to determine the global potential.

3. Solving: from analytical equations to numerical results

3.1. Analytical solutions

Analytical solutions of equations are often considered as the most valuable ones. Their numerical evaluation is direct and has almost no cost. They immediately give physically valuable information: how does that result behave when that parameter is changed, etc. They are not subject to numerical instabilities. They are also the subject of many school teachings for a long time before numerical methods are even addressed !

Unfortunately in most practical problems of interest to spacecraft plasma interaction, there is no analytical solution. The reason lies in the complexity of the equations and of the spacecraft geometry.

However, when the equation and/or the geometry is simplified, such solutions exist. They deal mostly with 1D geometry and/or simplified transport equations (linearised, only one species…). They give however good physical insight that proves very useful for a physical understanding of more complicated case. This is why we give a brief non-exhaustive overview of some of these results relevant to S/C plasma interactions. The interested reader shall look at the many existing plasma books for details [Chen, Chapman…].

The first and simplest of those analytical solutions is given in introduction of any plasma course. It is straightforward to show that a small (negative) potential is screened exponentially by a plasma with a decay length Langmuir length λ_D :

$$\phi(x) = \phi_{surf} e^{-x/\lambda_D} \quad , \quad \lambda_D = \sqrt{\varepsilon_0 k_B T_e / n e^2} \tag{24}$$

This solution relies on the following simplifications of the problem: constant ion density, Boltzmann density (18) for electrons, linearisation of Boltzmann exponential law for potential small compared to electron temperature (or close).

The second problem of interest is Child-Langmuir model. In 1D geometry again, considering one single charged species at zero temperature particles, the current between to planes is limited by space charge to a value called Child-Langmuir current, and the potential varies as $x^{4/3}$. That result can be applied to the region containing only the attracted species of a 1D sheath in case of a large surface potential ϕ_s. In that case the current is the thermal current that can be attracted from sheath edge, and the space charge limitation now determines the sheath size:

$$L = \frac{2(4\pi)^{1/4}}{3}\lambda_D\left(\frac{e\phi_s}{k_B T_e}\right)^{3/4} \sim 1.25\,\lambda_D\left(\frac{e|\phi_s|}{k_B T_e}\right)^{3/4} \quad (25)$$

which can now be much larger than Debye length.

In case of higher dimensionality the sheath size is no longer analytical, but some power law analytical fits of numerical results are reviewed in [Cooke 1996], along with some analytical results concerning S/C wakes.

Linearising fluid equations (14) is also the key to a third class of analytical computations: linear plasma wave analysis. The major difficulty of the non linear transport equations is circumvented by linearising them around a known solution (plasma at rest), a bit similarly to the first problem of the small potential sheaths (24), where Boltzmann distribution was linearised.

Some cases can also be solved analytically in spite of a more complex kinetic approach. One can cite kinetic sheath models with secondary emission in 1D planar geometry ([Stephens II and Ordonez, 1999] and references therein), and some Langmuir probe models (quasi 1D thanks to cylindrical or spherical symmetry, numerous publications).

3.2. Numerical solving methods

The power of numerical solving is that it can *a priori* cope with any geometry and any distribution function, contrarily to analytic solving. That may however be difficult or very time consuming in practice.

Kinetic modelling is especially costly since one must work in 6D phase space for a 3D modelling. Direct method consists in discretising (meshing) the velocity space like the distance space. The number of particles in each of these phase space cells is then stored in the 6D table. This is very costly in memory, and also CPU time, and in practice this is limited to lower dimensionality.

A kinetic modelling is however often required as was discussed in section 2: for ions that undergo few collisions, for electrons attracted by positive potentials, in case non Maxwellian injected distributions, etc.

The most popular kinetic modelling method is of Monte Carlo type. Particles representing many real particles are generated at random and moved according to single particle equations of motions through the electric field map that is stored on a mesh. Those particles generate a charge density on the mesh points close to them. The charge can be attributed to the Nearest Grid Point (NGP) are to all neighbouring points through a linear weighting (call called Particle-In-Cell, PIC) or higher order weighing (see the reference book [Birdsall and Langdon, 1985] for details). Then the field equations (mostly Poisson) are solved on that mesh, using those charges and the boundary conditions. The loop starts again with the particle moving.

The physicist may see that method as mimicking reality, with a large numbers of real particles of close position and velocity grouped within computer super-particles. The mathematician considers the super-particles as a way of representing the real distribution function *f* in phase space as a sum of Dirac singular distribution δ (the particle *i* of weight W_i contributes to $f_i(\vec{x},\vec{v},t)$ of the amount $W_i\delta(\vec{x}-\vec{x}_i(t))\delta(\vec{v}-\vec{v}_i(t))$). That sum of Dirac distributions is then naturally smoothed at the scale of the mesh cell.

That method is faster than direct method because some tens of particles per cell are usually used to represent the distribution function. This is enough for a crude description of a velocity distribution, and that description is improved over time thanks to the renewal of particles in a cell. Those Monte Carlo methods remain noisy (statistical fluctuations) and averaging over time is often necessary to get smooth densities. Moreover the random statistical noise only reduces as the square root of the number of particles. So, reducing it by increasing the particle number is very costly. Generating particles at regular space and velocity intervals (accordingly to probability) instead of purely at random allows yet to reduce the noise (see "quiet start" in [Birdsall and Langdon 1985] for details).

Fluid equations like (13) and (14) are usually solved by direct methods on space meshes. It is also possible to solve that kind of equations by particle methods (Smooth Particle Hydrodynamics, or Particle-In-Cell again), in which the sampling particles are a way of representing densities and fluxes (the physicist can view them as overlapping droplets). These particle methods for fluid equations allow to represent the transition between an expanding medium and vacuum more easily than direct methods, which have difficulties with vacuum. As Monte Carlo methods, they are noisy.

We discuss now specific issues related to numerical modelling. They were a bit arbitrarily grouped in time and space grid issues, but many have also to do with stability.

3.3. Time scale issues

The general scheme to compute time evolution of a plasma is the following. Transport is computed over a time step Δt in a given map of fields (by integrating either particle motion or fluid equations), then new densities and charge build-up on spacecraft are used to determine the new fields. Then the loop starts again. That can be called a Real Time (RT) computation. It allows to solve time dependent problems.

In such computations the integration time step is basically limited by the collective reaction time of particles. A new potential map must be computed before the density changes induce important changes in potential, which compels to stop transport integration. For electrons the integration time step Δt_e must thus verify

$$\Delta t_e \omega_{pe} << 1, \quad \text{with } \omega_{pe} = \sqrt{ne^2/\varepsilon_0 m_e} \tag{26}$$

where ω_{pe} is the electron plasma pulsation, the frequency of natural reactions or oscillations of electrons. Implicit methods (taking into account the potential changes generated by the integration over Δt to integrate over Δt) allow to increase that time step somewhat, but the order of magnitude remains.

When steady state solutions are searched for, a possible opposite method consists in computing the whole trajectories of particles on a given potential map, from the time particles enter the computation box to the time they come out of it, or are collected. Then, and only then, the charges generated by those trajectories are used to compute a new potential map, and then loop again. This may be called a Steady State Technique (SST).

It is approximately equivalent to using the previous RT method with a time step equal to the time of transit of particles through the mesh. It usually violates (26) unless the whole mesh is smaller than one Debye length (which is usually not the case, by definition if we are in "plasma situation", and not in a "charges in vacuum situation"!) That method is thus in general fundamentally unstable, and requires a large relaxation of the charge densities (use e. g. 99.9% of the density at step n-1 with just a small contribution of 0.1% of the newly computed density for step n) to recover stability. That may be very costly.

The theoretical (and practical) analysis of the general iterative charge relaxed Vlasov-Poisson problem in [Parker and Sullivan 1974] allows a good understanding on that problem. In that study, the relaxed Poisson-Vlasov iteration is written in the following form:

$$\Delta\Phi_{n+1} = \alpha F[\Phi_n] + (1-\alpha)\Delta\Phi_n \tag{27}$$

where Φ_n is the reduced potential field (in T_e units) at step n, $F[\Phi]$ is the reduced charge density (with opposite sign) which has a non-local non-linear dependence on the potential field and summarises in our case the result of the particle trajectory integration through the whole domain. The non-dimensional relaxation parameter α is between zero and one, but shall usually be small. The first term of right hand side is the density computed with the new potential Φ_n reduced by the small α parameter (relaxation), and the second term stands for the overall density used at previous step (write (27) with n replaced by n-1) normalised by 1-α. The (linear) stability of the iteration process $\Phi_n \rightarrow \Phi_{n+1}$ requires that no eigenvalue of the Jacobian of that transfer function from Φ_n to Φ_{n+1} be larger than 1 (in absolute value). Studying the eigenvalues of the Laplacian operator on a cubic mesh, it can be shown that this stability condition imposes

$$\alpha < \alpha_c \sim \frac{\beta}{L^2 \left| \frac{dF}{d\Phi} \right|} \tag{28}$$

where L is the total reduced mesh size (i. e. in Debye length units), $dF/d\Phi$ stands for an eigenvalue of the Jacobian matrix of the a priori unknown F functional (the largest is OK), and β is a numerical parameter depending on boundary conditions in the range of 15 to 60 in 3D (it summarises $2\pi^2/CK$ of equation (6) in [Parker and Sullivan 1974]). In general the computation box extension is many Debye lengths and L is large, which tends to make a very small relaxation parameter α, and to require of course many iterations (iteration number must be several times $1/\alpha$). It remains yet to determine the eigenvalues of the non-local dependence F of charge density as a function of potential. In case of a simple dependence like for drifting cold ions or Boltzmann electron distribution it can be easily computed and is of the order of 1 (remember those are reduced quantities, i. e. non-dimensional), or a bit smaller for ion kinetic energy much larger than T_e. Hence in general, for relevant meshes much larger than Debye length, the gain obtained compared to real time methods thanks to fewer potential computations and larger integration time steps is largely lost.

That method may however be suitable in specific more stable cases. For example deep within a sheath, accelerated particles have a density less sensitive to potential changes and the eigenvalues of F Jacobian in (28) become small. They can thus compensate for the large factor L^2 and allow to work with α not too small. That kind of Steady State Technique is indeed used in POLAR code for modelling sheaths [Lilley et al, 1989] and also NASCAP/LEO and DynaPAC [Cooke 1996]. It compels yet to use another technique outside the sheath (that method is unstable there in quiet plasma, unless very small relaxation parameter is used) and thus to explicitly handle the sheath boundary (sharp sheath approximation in POLAR).

It can be noted that a stabilisation technique different from charge relaxation is proposed in [Parker and Sullivan 1974] for the iterative solution of steady state Vlasov-Poisson problem. It is however close to Newton-type implicitisation (see next section below) and requires much information on the eigenvalues of the Jacobian of F, which is not available in general, especially when F is the result of a general Vlasov solver, and not known analytically thus.

Another time integration issue shows up when both ion and electron dynamics are to be modelled. Within one electron time step, ions move very little since their velocities are smaller typically by a ratio of square root of their mass ratio, that may be from 40 for protons to 500 for heavy ions. Many electron time steps are thus required to have the ions moved significantly. That enormous cost is the main reason why the use of a Boltzmann equilibrium density is so popular: it allows to skip the time scale of electron dynamics (its result is Boltzmann distribution) and to work at ion dynamics time scale. Other direct methods to determine electron densities (and fields) have the same enormous advantage, and should be used whenever possible: analytic computation of electron densities even with positive potentials in some simple geometries, Ohm's law in resistive plasmas (quasi-neutrality gives electron density, and their gradients gives electric field through Ohm's law), etc.

Let us note that the Steady State Techniques described above avoid that velocity ratio issue, but in general at the price of a very large charge relaxation, which may also be very costly.

When none of these direct or steady state methods is available, a first trick consists of making larger time steps for ions (sub-cycling) but the gain is of a factor of 2 at maximum when the computation cost for ions becomes negligible. This is very often insufficient. Another trick is to artificially reduce the ion to electron mass ratio to small unphysical values (e.g. $m_i/m_e = 100$ instead of 1836 or more). This is sometimes used as a test but cannot be of real use for space application since it induces unphysical biases.

The next possible idea is to get rid of the constraints of the physical time steps when one looks for steady states or slowly varying states. That was already the idea of the Steady State Technique described above, but the absence of reaction before the particles have crossed the mesh is excessive, and leads to instabilities in most cases: any potential deviation from the solution produces a density correction at next step over the whole domain (many Debye lengths), which in turn yields an even larger deviation of opposite sign for next computed potential. A more stable method consists in computing a time evolution like in the standard Real Time simulation described above (moving particle and computing fields when particles moved less than a cell) but with non-physical Numerical Times (NT) for electrons and ions: while electrons are moved of e. g. 1 μs, ions are moved of e. g. 50 μs, which allows them to move substantially in spite of their smaller velocity. Similarly to the Steady State Technique previously described, the steady state solution found by NT method is perfectly physical, even though the convergence to it is not, provided convergence happens! But contrarily to SST the dynamics is modelled in a "short loop": electrons and ions can react immediately to a potential fluctuation (they react only after a full crossing of the mesh in SST) and stabilise the scheme. Ions react faster than they do in reality (of a factor 50 in the example above), so it may generate unphysical transients, but the general stabilising reaction of the plasma is present. That method was applied to the modelling of the ROSETTA orbiter floating at a positive potential in a drifting comet plasma (see [Roussel and Berthelier, 2001] presented at that conference). Its application to the modelling of a sheath in presence of secondary emission [Jolivet and Roussel, 2001] was also successful although some non-physical instabilities showed up due to the Numerical Times method (well understood two-stream instabilities enhanced by the non physical dynamics of the ions). We discovered later that the method had already been used and described in detail in [Meyer and Wünner, 1997] where it was called Asynchronous Cycling. It may have been used elsewhere.

3.4. Space grid issues

A first issue concerning space meshing is that many different scales are involves. It goes from the small feature or device on a S/C to the S/C size. The whole sheath is also to be included in the computation box (quiet plasma assumption at boundaries) and it can be much larger than S/C in low plasma density (GEO, higher orbits, non terrestrial environments…).

The natural answer to that is to use a multi-scale mesh. It can be an unstructured mesh (irregular tetrahedra usually of very variable size). Building such 3D meshes is a bit difficult, but commercial software exit today. When Monte Carlo particle methods are used (PIC Real Time or Steady State), that kind of mesh has some extra cost in computing since determining in which cell the particle is has already some non negligible cost. Another method consists in using nested regular sub-meshes. The mesh of lower level has cells twice smaller than the embedding mesh.

Multi-scale meshes are very suitable to solve field equations on a large scale, but taking into account of particles remains a bit complicated: if the densities are similar everywhere, variable super-particle weights are to be used so that the number of super-particles in large cells remains reasonable. That requires some particle grouping or re-sampling at mesh boundaries.

Another solution to multi-scale problems consists in modelling only at the scale at which results are required, and handling other scales on an effective or empirical basis. This is mostly used for lower scale phenomena: reflection of electrons by a thin sheath in dense plasma, photo-sheath conductivity in GEO, plasma emission by a plasma device, collection by small areas (gap between solar cells e. g.), etc. can be very suitably taken into account thanks to appropriate analytical boundary conditions (particle source, reflection conditions, etc.). The larger scale physics can also be accounted for without using a real external mesh: potential conditions can be put in boundary conditions (for example mixed Dirichlet Neumann conditions for potential like (21) mimicking its $1/r$ behaviour in vacuum or $1/r^2$ in

plasma presheath in case of 3D spherical symmetry), while the incoming fluxes are to be modified accordingly to those non-rest conditions at external boundaries when possible (e. g. analytic models for spherical Langmuir probes, etc.).

The size of mesh cells is another important question. The basic "classical" criterion is that cells should be smaller than Debye length λ_D. There are two main reasons to that. First the potentials at a scale larger than λ_D should be screened, hence the interesting physics is at Debye length scale (or below). Second and most, cells larger than λ_D may generate instabilities: non neutrality at λ_D scale generates potentials of the order of T_e, so non neutrality at the scale of larger cells generates larger potentials and instabilities in many cases. That classical criterion for the cell size h

$$h < \lambda_D \tag{29}$$

together with the fact that particles should not cross more than one cell during one time step

$$v_{i/e}\Delta t_{i/e} < h \tag{30}$$

is perfectly consistent with the time step criterion (26) since (29) and (30) give (26) when using electron thermal velocity.

It is however common now to go beyond these limitations. It is first often necessary, because there may be physics of interest at scales larger than λ_D, for instance in case of large potentials on S/C (see e. g. Child-Langmuir 1D sheath size (25) much larger than λ_D). Using such large cells is then possible, thanks to implicit methods. When modelling electron dynamics implicit methods allow to go beyond (26) and (29) simultaneously. When using a macroscopic law as the result of electron dynamics (Boltzmann distribution, Ohm's law…), the electron time step is no longer considered, and impliciting those laws allows to go to larger cells.

We detail a little bit the case of Boltzmann distribution for the electrons that is of very common use. It will also show the general principle of implicit methods. The explicit problem of solving Poisson equation with a Boltzmann distribution for the electrons is the following:

$$-\Delta\Phi_{n+1} = n_{ion} - \exp(\Phi_n) \tag{31}$$

for non-dimensional quantities, with a given ion density n_{ion}, and a Boltzmann electron density depending on the potential Φ. The potential Φ_n at previous step n is used to compute electron density. This is a particular case of the iterative problem stated in (27) where no relaxation is envisaged ($\alpha = 0$) and where the form of the dependence of density on potential is known (fixed for ions + exponential dependence for electrons). Hence the same kind of theoretical linear analysis as in [Parker and Sullivan 74] applies. The eigenvalue of the Jacobian of the charge density law $dF/d\Phi = d(\exp(\Phi))/d\Phi = \exp(\Phi)$ is of the order of 1 in small potential regions. Linearising (31) around the solution shows that a perturbation $\delta\Phi$ with Laplacian eigenvalue λ_L gets at next step

$$\delta\Phi_{n+1} = \delta\Phi_n / \lambda_L \tag{32}$$

Laplacian eigenvalues are k^2 for eigenvector $\delta\Phi = \cos(kx)$, with the minimum value for k close to one over the box size (perturbation wave length is the box size). The iteration is thus divergent as soon as the total size of the system is larger than λ_D! In practice however those long wave perturbations do not easily show up, either because they are difficulty excited or because they are damped due to the non linear behaviour of exponential law (for negative potentials at least, and a cut-off is usually used for positive potentials). Remember this is only a linear analysis. In practice shorter wave length show up for which Laplacian has larger eigenvalues. This scheme becomes thus divergent when Debye length is smaller than a couple of cells.

Since we want to have Debye length smaller than one cell, much progress is still needed. This is done by the implicit scheme. The exact solution would be obtained in one step by solving

$$-\Delta\Phi_{n+1} = n_{ion} - \exp(\Phi_{n+1}) \tag{33}$$

but this is a non-linear transcendent equation that cannot be solved directly. Hence the implicit scheme consists in approximating (33) through a linearisation of the exponential

$$\exp(\Phi_{n+1}) \sim \exp(\Phi_n) + (\Phi_{n+1} - \Phi_n)\exp(\Phi_n) \tag{34}$$

which gives the tractable linear equation

$$-\Delta\Phi_{n+1} - \Phi_{n+1}\exp(\Phi_n) = n_{ion} - (1 - \Phi_n)\exp(\Phi_n) \tag{35}$$

for that implicit scheme. Linear analysis shows that small perturbations around the solution are always damped (stability). Since the exponential is not linear, problems may still arise for large perturbations towards positive potentials, and some correction methods may be applied then [Parker 1977].

That can of course be applied to any charge distribution as a function of potential (non Boltzmann). Implicit methods have of much larger scope and are very powerful when a system is strongly self-coupled. It the framework of S/C-plasma interactions they can be used to integrate currents on surfaces when those currents depend sharply on potentials, to model the electron dynamics with larger time steps by estimating the potential change induced by their own movement, etc.

4. Examples

Three common plasma environments are addressed here: the natural GEO and LEO plasma, and the artificial plasma environment induced by electric propulsion (EP), which is of a more and more frequent use on spacecraft. For each of them the physics of that environment is briefly sketched as a necessary base before describing the specificities of its modelling.

4.1. GEO

4.1.1. The environment and the physics in brief

In geosynchronous orbit, the plasma density is very low. Densities found in literature are in the range of 1 to 100 cm^{-3} for the cold plasma at temperature around 1 eV, and around 1 cm^{-3} for the very variable hot plasma of temperature 10 to 100 keV during sub-storms.

The Debye length, dominated by the cold plasma, is thus in the range of 1 to 10 meters. The typical currents that may be collected or emitted by spacecraft surfaces are summarised in table 2. The physics is thus dominated by energetic electrons (during sub-storms) and photo-emission.

Collected thermal electrons	Collected hot electrons	Collected thermal ions	Emitted photo-electrons
~ 10 pA/cm^2	~ 1 nA/cm^2	~ .1 pA/cm^2	~ 5 nA/cm^2

Table 2- typical currents on S/C in GEO

We also recall the typical behaviour of spacecraft during storms. They charge negatively due to energetic electrons (hot plasma), and the photo-emission is generally not able to cancel that charging because a potential barrier builds up in from of the sunlit surfaces due to the more negative potentials on the shaded sides, as it can be seen on the drawing below.

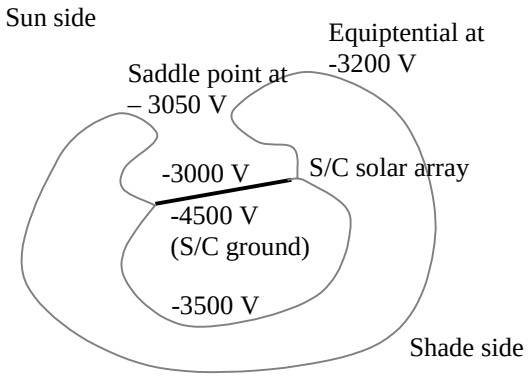

Figure 1- typical potential barrier (or saddle point) situation in GEO

4.1.2. Modelling: possible approximations

In GEO, the Debye length is comparable to S/C size. Moreover the S/C potentials are large, which results in a sheath much larger than S/C (see 3.1 and (25)). The drastic simplification that is thus possible is to completely ignore the plasma density to solve Poisson equation. This is for example done in NASCAP. That does not mean of course ignoring current collection on surfaces.

Since Debye length is similar to S/C size, and although sheath extension is much larger than S/C size, that simplification may change somewhat the quantitative values (the general qualitative results with potential barrier is not put into question yet). The consequence of taking into account the plasma density (mostly cold ions, either coming onto the S/C or going back after an open orbital trajectory) would be some potential screening. That would lead to larger fields on the S/C, thus to a larger capacity and above all to a reduced potential barrier effect, hence to a larger differential charging. That effect might be small but would be worth testing.

That simplification is of course enormous since field equations and particle movement are uncoupled, at least in volume. The charged particles are moved in fields that do not depend on the densities they generate (energetic electrons of tens of keV may even be moved without electric field considerations). This is no longer considered as a plasma situation but as a "charges in vacuum" situation. The charge-potential coupling still exists through the collection of charges by S/C, which generates surface potentials, and thus volume potentials, but is not as complex as the general Vlasov-Poisson coupling.

4.1.3. Practical difficulties

So, in GEO, the usually difficult problem of the strongly coupled non-linear Vlasov-Poisson equations does not exist. Some difficulties do exist yet. They have much to do with multi-scale issues either in time or in space, similar to some discussed in 3.3 and 3.4 sections above.

The absolute capacitance of S/C in GEO is much smaller than the capacitance of its dielectric coatings (coverglasses…): a fraction of nF versus several μF. Hence the time scale for absolute potential charging is much smaller than the time scale for relative charging between the mass and the sunlit coverglass: typically tens of milliseconds versus hundreds of seconds. Crude numerical integration should use time steps at the scale of the millisecond, during which the absolute potential changes little. But integrating over hundreds of seconds would then be costly. Fortunately implicit methods (see 3.4 for an example of implicit method) allow to integrate with time steps closer to the large time scale of differential charging: the potential at next iteration step is taken into account to compute the current until next step. This is implemented in NASCAP.

The other difficulty has to do with multi-scale in space. First, the large Debye length and large potentials in GEO induce large sheaths (hundreds of meters). This can be handled thanks to larger meshes containing the smaller mesh at S/C scale (NASCAP), or also by using appropriate mixed Dirichlet-Neumann conditions to mimic asymptotic spherical potential behaviour at some distance of S/C (see 3.4), for example around 20 meters, although that does not allow to follow emitted electrons beyond that limit. On the opposite side, small scale volume phenomena may be important: photo-sheath of re-collected photo-electrons, local potential gradient at dielectric/conductor/vacuum triple points that are risks of electrostatic discharges (ESD), current collection by small surfaces (e. g. interconnectors), influence of potentials in intercellular gaps on currents onto coverglasses, etc. The best way to take these phenomena into account is through an empirical description. Meshing at their small scale would be required on a whole spacecraft, which would be too costly. Their empirical description can yet be obtained through a (single) numerical modelling (that e. g. gives the current enhancement factor for a collection by a small biased surface in given conditions).

In spite of those local phenomena, the general GEO S/C modelling is relatively simple from a point of view of volume effects, since space charge can be neglected. Most of the difficulty is transferred on the surface modelling with many surface phenomena to be taken into account (see 2.1.3.2 or NASCAP information). There is a great difference between volume and surface phenomena. Volume phenomena involve simple physics (basically electrostatics and particle motions) and difficult modelling (non-linear strongly coupled Vlasov-Poisson equations). Surfaces phenomena involve much more difficult physics (particle-matter interactions, induced conductivity…) which turns out eventually to be easy to model, since it is taken into account empirically, through coefficients taken from experiment. So, in GEO a large part of the difficulties is transferred to the experimenters! Hence we shall let them discuss the measurement issues of all of those parameters. We may just warn the modeller that many parameters are not well known since they require a very large experimental work on many different materials. Moreover, some of them are very sensitive to surface state (secondary emission is very sensitive to contamination…). Of course, those comments on modelling simplicity in GEO only deal with the situation under study here: quasi-static charge build-up. They are not valid for model predictions of ESD triggering, which depends on more complex volume and surface physics at a microscopic scale.

4.2. LEO

4.2.1. The environment and the physics in brief

In low earth orbit, the plasma density is higher than in GEO, with densities in the range 10^4 cm^{-3} to 10^6 cm^{-3}, and sometimes down to 10^3 cm^{-3} in auroral zones crossed by Polar Orbits (PEO). Typical temperatures are 1000 to 2000 K. The Debye length ranges thus from millimetres to centimetres. The energetic electrons trapped in the radiation belts produce currents negligible when compared to the cold plasma thermal currents. Such is not necessarily the case for auroral electrons that may impinge S/C in plasma depleted auroral regions. The typical currents that may be collected or emitted by spacecraft surfaces are summarised in table 3. The last row dealing with auroral regions shows a risk of charging in those zones.

	Collected thermal electrons	Collected auroral electrons	Collected drifting ions	Emitted photo-electrons
LEO	10 - 1000	-	0.1 - 10	5
PEO	1	up to 5-10 very transiently	0.01	5

Table 3- typical currents on S/C in LEO and in plasma depleted auroral zones crossed in PEO (assumed 10^3 cm^{-3}), currents in nA/cm^2

The main origins for large potentials are thus the following in low earth orbits: charging in auroral zones (hundreds of Volts negative have been measured), active device or power supply voltage (electrical power is produced at almost 200 V on ISS), tethers (due to the electromotive force when the tether crosses magnetic field lines).

Other remarkable phenomena show up on wake side of S/C. Due to the mesothermic flow (supersonic ions and subsonic electrons in S/C frame), the wake is ion depleted. First, that yields moderate negative volume potentials in the wake. Then, ions cannot be collected on wake surfaces of S/C. Dielectric surfaces in the wake are thus the surfaces reaching high negative potentials in the auroral zones most easily.

4.2.2. Practice: possible approximations, difficulties

Floating potentials on a passive body are a couple of times the electron temperature negative. In such a case the extension of the sheath is close to Debye length, typically centimetres. Its extension is also small in case of relatively small positive potentials, that may show up on the most positive part of solar arrays. The sheath extension can then be neglected, and the sheath handled as a simple boundary condition.

In case of a negative floating potential, the ions can thus be assumed to be collected and most electrons reflected. The potential drop coming from current balance can be approximated by (see e. g. [Chapman])

$$\phi_{\text{surf}} - \phi_{\text{plasma}} \sim -\frac{k_b T_e}{2e} \ln\left(\frac{m_i}{2\pi e^{-1} m_e}\right) \sim -\frac{k_b T_e}{2e} \ln\left(\frac{m_i}{2.3 m_e}\right) \tag{36}$$

from total current balance on an insulated surface (or isolated body) for Maxwellian electrons and a cold ion current entering the sheath after acceleration up to Bohm criterion by the presheath from a plasma at rest at a large distance. This is valid for walls parallel to S/C velocity, and a correct formula for ram facing walls is

$$\phi_{\text{surf}} - \phi_{\text{plasma}} \sim -\frac{k_b T_e}{e} \ln\left(\sqrt{\frac{k_b T_e}{2\pi m_e}} \Big/ V_{S/C}\right) \tag{37}$$

which takes into account ion drift at S/C velocity $V_{S/C}$. The electron collected currents follow from the same analysis.

If the current balance involves collection by small parts of S/C, like collection by interconnectors for S/C global current balance, a very local simulation at the scale of solar cells is to be performed to assess the enhancement of collection by ion or electron focussing. It may then be used as an empirical collecting model for interconnectors or any other pinhole in a coating.

All of that makes the modelling of “standard situations” in LEO, i. e. without charging, rather straightforward. A specific treatment may only be required for the electron collection by the positively biased part of solar arrays or other devices (analytic approximation thanks to Langmuir probe models, local numerical modelling…), but the whole computation can almost be handled analytically without numerical modelling (putting together all currents that led to formulas (36) and (37), all over S/C).

The interest of modelling such “standard situations” in LEO is however limited. Standard S/C with low voltage electrical supply encounter no problem: their ground floats some tens of Volts negative and the most positive part of their solar arrays floats some (tens of) Volts positive.

The issue is more serious for higher voltage power supplies, like ISS. That may induce floating potentials of the order of –150V (which lead to take a plasma contactor onboard ISS to avoid the subsequent ESD and sputtering risks). In such an “interesting” situation those potentials are around a thousand of times larger than T_e and produce large sheaths (decimetres to metres according to the Child Langmuir law (25) for 1D sheaths).

We are thus coming to non trivial cases, when large potentials arise on S/C and produce large sheaths. That happens in case of large voltage power supply, of charging in auroral regions, of tethered systems, etc. When large sheaths develop on scales similar to the ones of S/C, simple analytical formulas can no longer be used because of the focussing of the attracted species. Extra complications show up due to the drift of ions, which further reduces the possibilities to use analytic formulas for sheaths, and due to the magnetic field in case of electron collection by positive potentials (ion gyration radius is large and ion collection can be considered as an unmagnetised phenomenon).

However some analytical work is still possible. In case of collection by probes in a magnetised plasma analytical results for the collected current exist [Parker and Murphy 1967]. Currents measured in flight on the Tethered System were higher than predicted yet, certainly due to pre-sheath turbulence and heating not present in the Parker-Murphy model [Cooke and Katz, 1998]. The density of attracted (and focussed) ions is also used in an approximated analytical form in POLAR, NASCAP/LEO and DynaPAC models (see their manual users or e. g. [Mandell et al, 1991]).

Returning to the general scheme for modelling high potentials on LEO S/C, it clearly requires the explicit numerical modelling of (large) sheaths. We discuss briefly the main features of such a modelling, since most of have already been discussed in section 3.

Potential profiles at small scale lengths as e. g. sheath or wake edge that can be at Debye length scale (~1 cm) cannot be easily modelled with a mesh at S/C scale. Modelling such edges with a decimetre coarse resolution (cells of 10 cm e. g.) essentially results in a smoothing of that edge at cell scale, with a subsequent inaccuracy on potential at that scale also.

When only negative potentials or involved, Boltzmann equation is usually used for cold electrons. Using an implicit Boltzmann-Poisson solver (see 3.4) stabilises the iterative Vlasov-Poisson scheme and allows to use cells larger than Debye length.

When electron dynamics must really be modelled due to positive potentials (tethers, active bias), stability issues become more acute while computation time issues arise due to very different velocities for ions and electrons. Stability can be achieved through relaxation or implicit techniques, while computation time is reduced by steady state or numerical time techniques (see 3.3).

A more “technological” improvement was implemented in NASCAP/LEO, POLAR and DynaPAC code series, where the boundary of the sheath and pre-sheath is explicitly computed. That allows to use different modelling in the sheath, and in the pre-sheath (analytical ion density or not, steady state or PIC method…). That certainly improves computation time and stability, at the price of extra complexity, coding time, and sharp edge approximation between sheath and pre-sheath.

4.3. Electric Propulsion

4.3.1. The induced environment in brief

The environment produced by electric thrusters is first described briefly. By electric thruster, we mainly mean Hall thruster (SPT, Stationary Plasma Thruster) or ion engine (gridded, principle similar to Kaufmann source), although other thrusters may have partially similar effects (Arcjets, MPD, FEEP, PPT…).

The primary effluents are of such thrusters are:

- Fast accelerated ions: typically xenon at 300 or 1000 eV for Hall and ion thrusters respectively
- Non ionised neutrals: typically some percents of xenon
- Products of thruster erosion by fast ions: ceramics of SPT walls (often $BNSiO_2$) or grids of ion engines (Molybdenum, Carbon…).

The dynamics out of the thruster itself, i. e. in the plume and on S/C surfaces, first involves collisions:

- Charge exchange (CEX) collisions, mainly in the near field plume, since they are proportional to both decreasing ion and neutral densities: $Xe^{+}_{fast} + Xe_{slow} \rightarrow Xe_{fast} + Xe^{+}_{slow}$
- Elastic collisions (and others), mainly in the near field plume again: cross sections are a decade smaller than CEX
- Impingement on S/C surfaces produces sputtering. The sputtered atoms/molecules are potential sources of contamination through re-deposition elsewhere.

It also involves collective plasma behaviour:

- The presence of a dense plasma in the plume and also all around S/C due to the spreading of the cold plasma generated by CEX (~10^{10} cm^{-3} at SPT exit down to densities typical of LEO in outer regions of the plume)
- The ordinary consequences of the presence of relatively dense plasma: capability to conduct currents, current leakages, capacity discharging, potential screening… In particular an electric thruster is considered to act as a plasma contactor and discharge relative and absolute potentials thanks to the induced plasma conductivity.
- Electromagnetic and plasma noise on a wide frequency spectrum (oscillations of SPT around 20 kHz, higher frequency noise…).

4.3.2. Modelling: possible approximations

Due to the recent great interest in Electric Propulsion (EP), many studies were performed and published in the last five or ten years. We will stick to the modelling principles here.

A first basic approach concerning fast ions is to assume they are little affected by the 20 to 40 Volts of potential existing in the plume. They follow straight lines and their impingement on S/C surfaces (essentially on solar array in north-south station keeping configurations envisaged GEO) can be computed by simple ray tracing. The angle and energy distribution functions of ions are taken from experiments in the vicinity of thruster exit (decimetres to 1 meter

usually). That simple approach is rather valid as long as high energy ions are concerned, but misses the cold plasma generated by CEX.

The next widespread approach is to make a standard PIC modelling of ions including CEX for the generation of cold plasma. Since experimental measurements show that the electron distribution function in the plume is close to Maxwellian with a rather homogeneous temperature (with some temperature gradient approximately from 2 to 5 eV at most), almost all modellers assume an isothermal Boltzmann electron distribution. The advantages of using isothermal Boltzmann distribution are so important (simplicity, rapidity, stability…), that this reasonable simplification is understandable. However it is directly at the origin of the predicted potentials in the plume, since Boltzmann distribution and quasi-neutrality yield the following potential as a function of density

$$\phi(\vec{x}) = \phi_0 + \frac{k_b T_e}{e} \ln\left(\frac{n(\vec{x})}{n_0}\right) \tag{38}$$

(potentials can in fact be obtained directly from that formula when no space charge region exists, which is sometimes called the plasma approximation). The potentials in the plume appear thus to be directly proportional to T_e and that approximation reduces somewhat their accuracy.

The CEX collisions between ions and neutrals can be modelled either by assuming a fixed "background" neutral density (unaffected by those collisions), or by also modelling the effect of those collisions on the neutral density through a more accurate and complex Direct Simulation Monte Carlo (DSMC) for example. The difference looks to be small, since indeed the neutral density is little affected by the CEX collisions in the plume.

4.3.3. Results and comments

Due to the Boltzmann distribution used, or equivalently to Eq. (38) the potentials in the plume are a couple of T_e away from the surrounding environment (e. g. 14 T_e for 6 decades in density). Typical temperatures of T_e 1 to 5 eV yield tens of Volts between plume centre and surrounding CEX generated plasma.

As a first consequence, accelerated CEX ions are thought to produce no or little sputtering on S/C. The second consequence is that such small potentials have little effect on fast ions, as stated previously. On the one hand that justifies the basic modelling of fast ions by straight-line ray tracing, but on the other hand that means that concerning fast ions, one approximately gets in the plume far field what one used as input in the plume near field. That emphasises the importance of the fast ion distribution function used as sources in such models, especially at large divergence angle (~60°) where ions may impinge S/C solar arrays, but are not very well characterised experimentally on ground.

This is however important essentially for non-charging effects like forces and torques computations, sputtering and subsequent contamination. The major effect concerning charging is that the CEX generated dense plasma spreads all over the S/C and discharges any relative or absolute potential. That requires first to model the CEX phenomenon, and then to correctly model the expansion of the cold plasma produced (quasi-neutrality leading to (38) cannot be maintained at very small density, e. g. on S/C side opposite to the thruster, as e. g. zero ion density leads to infinity in (38)). Even though electron Boltzmann distribution is approximate, the qualitative plasma contactor behaviour of the thruster (i. e. the capacity to furnish large currents) is corrected modelled this way.

A more difficult issue is related to a pre-charged S/C in GEO. The discharging of the absolute and relative potentials is granted due to the plasma contactor effect, but whether it shall be smooth or disruptive may still be questioned. Since microscopic ESD ignition is not yet accurately modelled to reach a predictive character, pretending from pure modelling results that the arrival of a dense thruster plasma on differential potentials will lead to their smooth discharging is certainly abusive. The triggering of an avalanche by the incoming dense plasma may still be feared, as long as a perfect understanding and modelling capability of the ESD ignition is not developed.

5. Conclusion

General and specific equations were described. Numerical methods for solving them were discussed. Their possible applications to three situations of common interest, GEO, LEO and EP environments, were reviewed.

The physical validity of the results was always the guiding principle for choosing or possibly simplifying the equations. When the modeller comes to that final step of physical validation, he should remember that two steps are to be validated. First, did the chosen equations correctly model reality ? Secondly, were the equations correctly solved ?

The comparison of simulation results with analytical results or other code results only validate the second step. Real validation can only arise through comparison to experimental data, that validates both equations and their solving. The dark side of experimental validations is that they can sometimes lack of generality and accuracy on each step, due to their global character. In particular they are not always well suited to check the accuracy of equation solving, since the experimental data are often the "results" of more complex physics than the simplified equations solved in the simulation. Those comments should of course not be understood as restricting the necessity to go through experimental validation to estimate the overall validity of simulation results.

References

Bernstein, I. B., and Rabinowitz, I. N., "Theory of Electrostatic Probes in a Low Density Plasma", *Physics of Fluids*, Vol. 2, No. 2, 1959, pp 112-121.

Birdsall, C. K., and Langdon, A. B., Plasma Physics via Computer Simulation, New York: McGraw-Hill, 1985.

Chapman, B. , Glow Discharge Processes, John Wiley & Sons, New York, 1980.

Chen, F. F., Introduction to Plasma Physics, Plenum Press, New York, 1974.

Cooke, D. L., Wake effects in spacecraft charging, *Space Environment Prevention of Risks Related to Spacecraft Charging*, Cépaduès Editions, Toulouse, France, June 1996, pp 271-288.

Cooke, D. L., and Katz, I., TSS-1R electron currents: Magnetic limited collection from a heated pre-sheath, *Geophysical Research Letters*, Vol. 25, No 5, March 1998, pp 753-756.

Jolivet, L., and Roussel, J.-F., Numerical Simulation of Plasma Sheath Phenomenon in Presence of Secondary Electronic Emission, submitted to *IEEE Transactions on Plasma Science*, 2001.

Lilley, J. R., Cooke, D. L., Jongeward, G. A., and Katz I, POLAR User's manual, Geophysics Laboratory, Hanscom, GL-TR-89-0307, October 1989.

Mandell, M. J., Jongeward, G. A., and Cooke, D. L., Spacecraft-plasma interaction codes: NASCAP/GEO, NASCAP/LEO, POLAR, DynaPAC, and EPSAT, *Fifth Annual Workshop on Space Operations Applications and Research*, Houston, Texas, July 9-11, 1991, pp 672-679.

Meyer, P., and Wünner, G, Asynchronous cycling as convergence acceleration method in particle simulation of direct current flow discharge, *Phys. Plasma*, Vol. 4, No 9, Sept. 1997.

Parker, L. W., and Murphy, B. L., Potential buildup on an electron emitting ionospheric satellite, *Journal of Geophysical Research*, Vol. 72, No 5, March 1967, pp 1631-1636.

Parker, L. W., and Sullivan, E. C., Iterative Methods for Plasma-Sheath Calculations - Application to Spherical Probe, Goddard Space Flight Center, MD, NASA TN D-7409, March 1974.

Parker, L. W., Calculation of Sheath and Wake structure about a Pillbox-Shaped Spacecraft in a Flowing Plasma, *Proceedings of the Spacecraft Charging Technology Conference*, AFGL-TR-77-0051, NASA TMX-73537, 1977.

Quémada, D., Ondes dans les plasmas, Herman, Paris, 1968.

Roussel, J.-F., and Berthelier, J.-J., Numerical Simulation of the Electrical Charging of the ROSETTA Orbiter, 7th *Spacecraft Charging Technology Conference*, Noordwijk, The Netherlands, April 23-27, 2001.

Stephens II, K. F., and Ordonez, C. A., Sheath and presheath potentials for anode, cathode and floating plasma-facing surfaces, *J. Appl. Phys.*, Vol. 85, No 5, March 1999, pp. 2522-2527.